A comparative study on the mechanisms of anti-lung cancer activities of three sulfated galactofucans

Wenjing Zhang[a, #], Wanli Wu[b, #], Yizhong Bao[c], Xiaojun Yan[d], Fuming Zhang[e], Robert J. Linhardt[e, f], Weihua Jin[b, e] * and Genxiang Mao[c] *

[a] Department of Endocrinology, Sir Run Run Shaw Hospital, Zhejiang University School of Medicine, Hangzhou, 310016, China
[b] College of Biotechnology and Bioengineering, Zhejiang University of Technology, Hangzhou 310014, China
[c] Zhejiang Provincial Key Lab of Geriatrics, Department of Geriatrics, Zhejiang Hospital, Hangzhou 310013, China
[d] Marine Science and Technical College, Zhejiang Ocean University, Zhoushan, 316022, China
[e] Department of Chemical and Biological Engineering, Center for Biotechnology and Interdisciplinary Studies, Rensselaer Polytechnic Institute, Troy, NY, 12180, USA
[f] Department of Biological Science, Departments of Chemistry and Chemical Biology and Biomedical Engineering, Center for Biotechnology and Interdisciplinary Studies, Rensselaer Polytechnic Institute, Troy, NY, 12180, USA

Supplementary data

1.1 Preparation of SGF and its derivatives [1]

After decolorizing with 85% ethanol for three times，the brown algae *Sargassum thunbergii* (100 g) was treated with hot water (3 L) for 4 h. The extract solution was then filtered with celite to remove residue and then concentrated by distillation under reduced pressure. Further elimination of alginate was achieved using 20% ethanol with $MgCl_2$ (0.05 mol/L). The solution was then concentrated and crude polysaccharide was obtained by ethanol precipitation.

Crude polysaccharide (6 g) underwent anion exchange chromatography on a

DEAE-Bio Gel Agarose FF gel (6 cm × 40 cm, Zhengguang, Hangzhou, China) with elution by water (5 L), 0.5 M NaCl (5 L) and 2 M NaCl (5 L). The polysaccharides were then dialyzed, concentrated, and precipitated by ethanol. Fraction eluted with 2 M NaCl was named SGF.

SGF (5 mg/mL) was converted to the H^+ form and left for 72 h at room temperature. After neutralization, concentration and precipitation, using a 10-fold excess of methanol, the methanol precipitate was named SGF-H and the supernatant was concentrated again and precipitated by 6-fold ethanol. The ethanol precipitate was named SGF-L and the supernatant was named as SGF-S.

A 100 μL portion of SGF-S (100 mg/mL) was separated with SuperdexTM peptide 10/300 GL column with elution in 0.2 M NH_4HCO_3 at a flow rate of 0.4 mL/min. Then, the eluates were collected and lyophilized to obtain different sulfated oligomers.

1.2 Mass spectrometry and nuclear magnetic resonance spectroscopy analysis

Electrospary ionization mass spectrometry (ESI-MS) and tandem mass spectrometry (MS/MS) were performed on a LTQ ORBITRAP XL (Thermo Scientific, Waltham, MA, USA). The samples were dissolved, centrifuged and analyzed. Mass spectra were registered in the negative ion mode at a flow rate of 5 μL/min. The capillary voltage was set to −3000 V, and the cone voltage was set at −50 V. The source temperature was 80 °C, and the desolvation temperature was 150 °C. All spectra were analyzed by Xcalibur.

Polysaccharides (30 mg) were deuterium oxide (99.9%) exchanged twice before dissolving in deuterium oxide (99.9%). Nuclear magnetic resonance (NMR) spectra were recorded on a Bruker AVANCE III 600 MHz (Billerica, MA) at 25°C. NMR spectra were recorded at a Hudson-Bruker SB 800 MHz spectrometer (Bruker BioSpin, Billerica, MA, USA) at 25 °C.

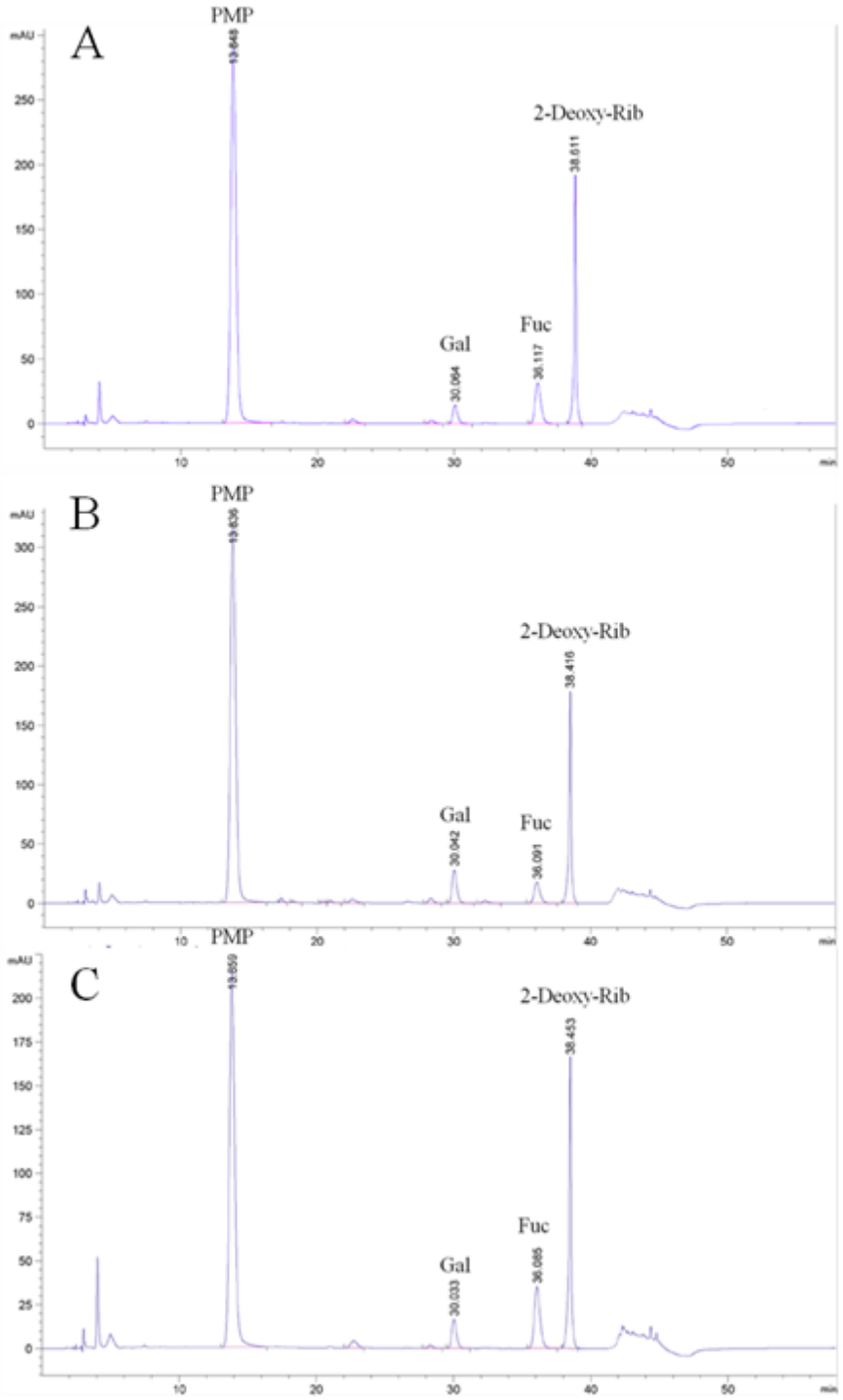

Figure S1. The PMP derivatization-HPLC spectra of SGF (A), SGF-H (B) and SGF-L (C).

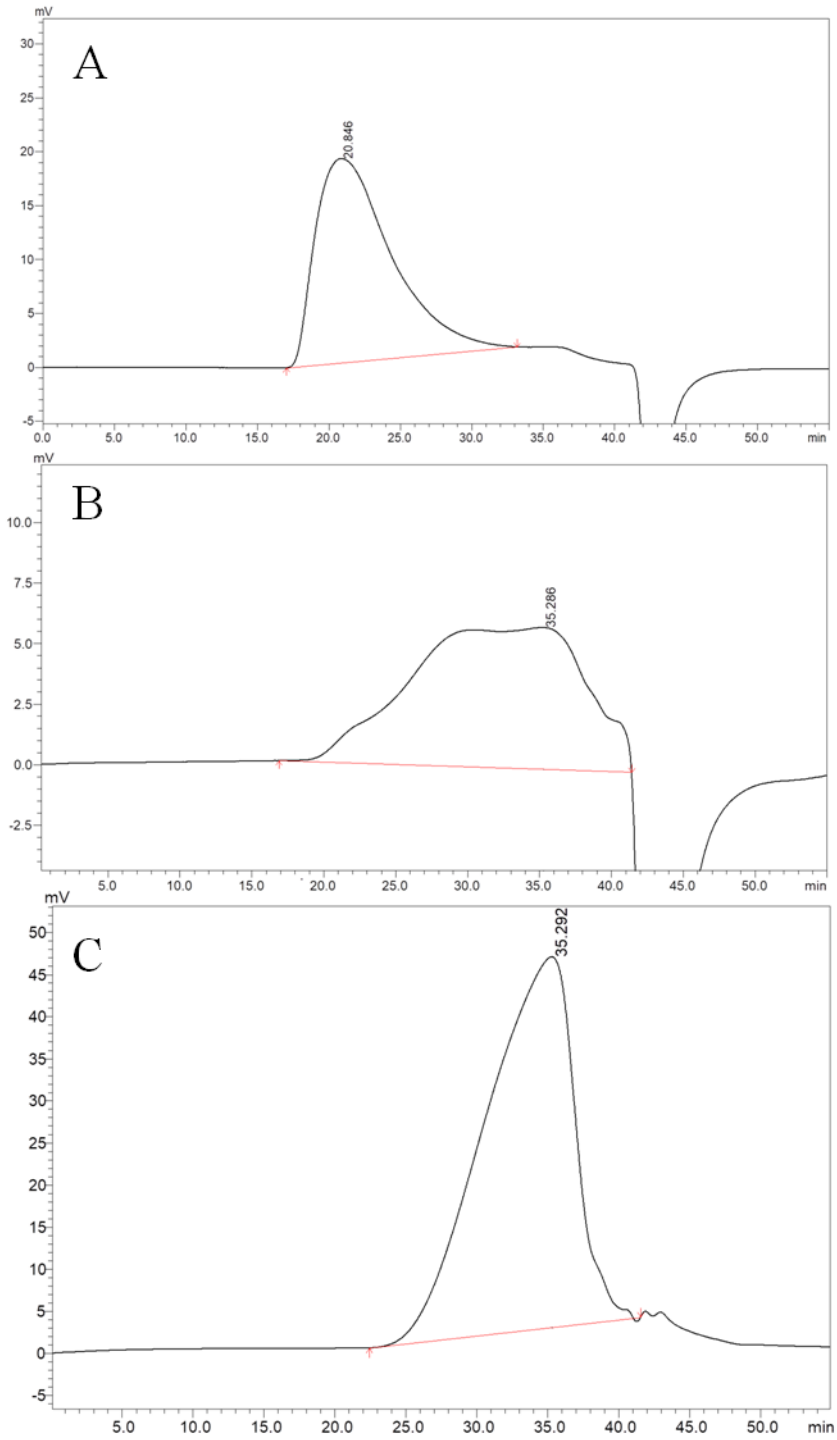

Figure S2. The GPC-HPLC spectra of SGF (A), SGF-H (B) and SGF-L (C).

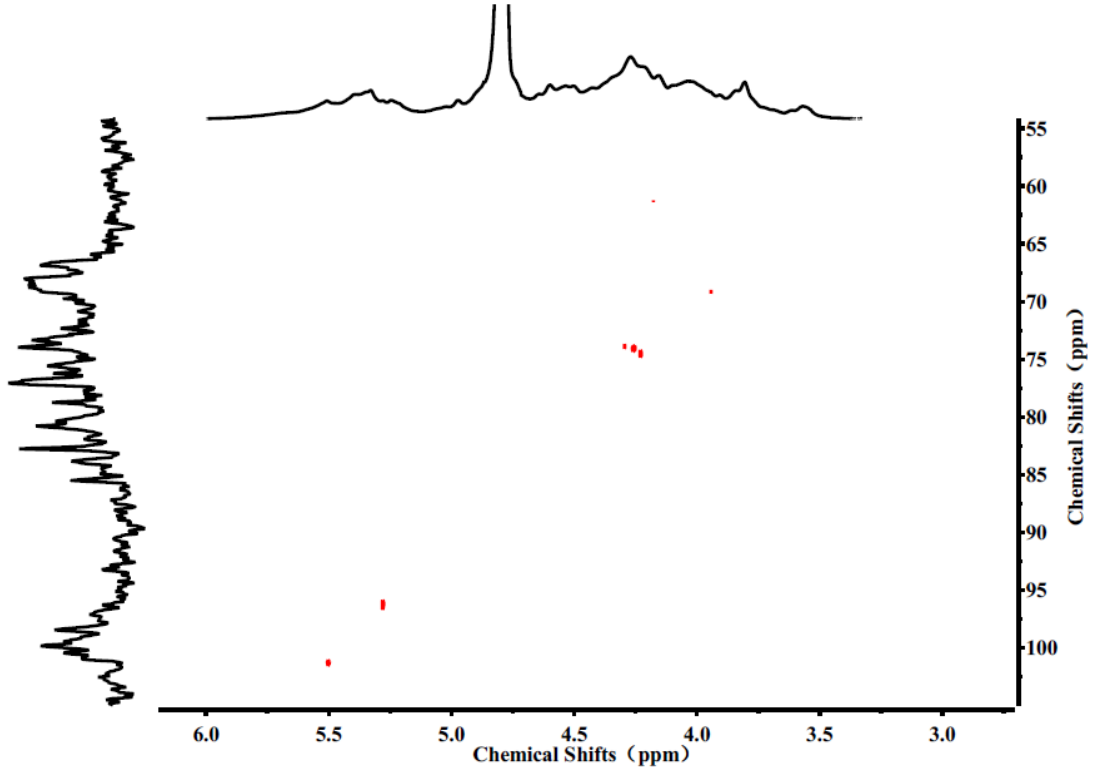
55
60
65
70
75
80
85
90
95
100
Chemical Shifts（ppm）
6.0
5.5
5.0
4.5
4.0
3.5
3.0
Chemical Shifts（ppm）

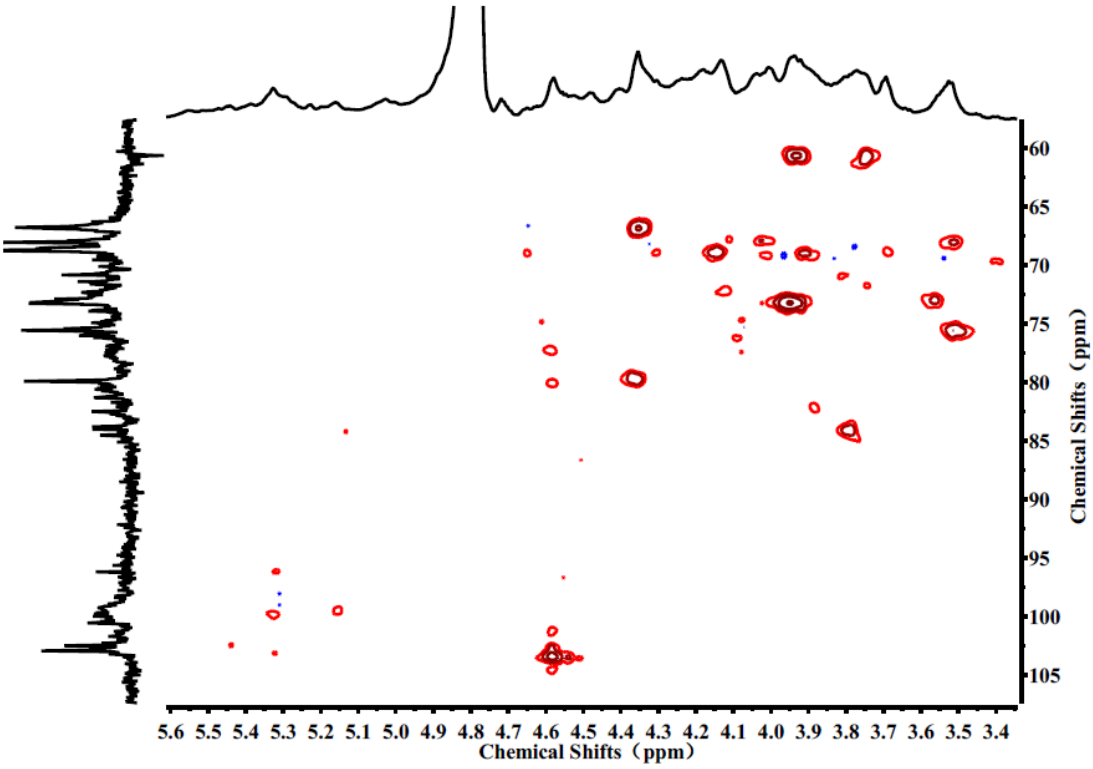
60
65
70
75
80
85
90
95
100
105
Chemical Shifts（ppm）
5.6 5.5 5.4 5.3 5.2 5.1 5.0 4.9 4.8 4.7 4.6 4.5 4.4 4.3 4.2 4.1 4.0 3.9 3.8 3.7 3.6 3.5 3.4
Chemical Shifts（ppm）

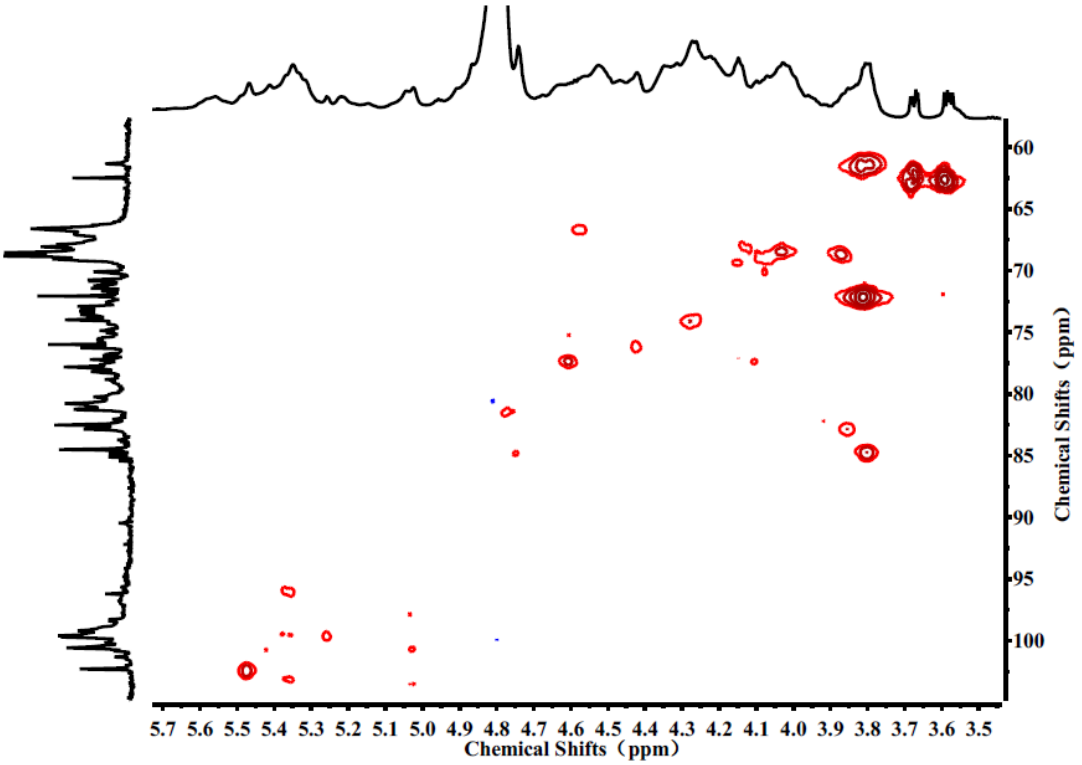

Figure S3. The HSQC spectra of SGF, SGF-H and SGF-L (From top to bottom).

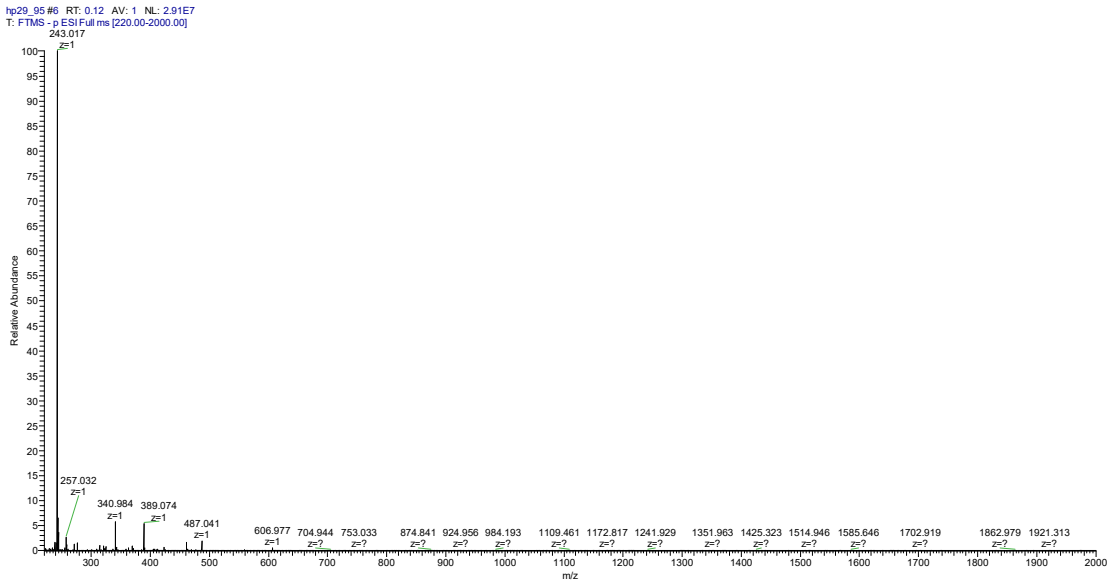

Figure S4. Negative-ion mode ESI-MS spectrum of Fraction 1 (Collected from 44-45 min).

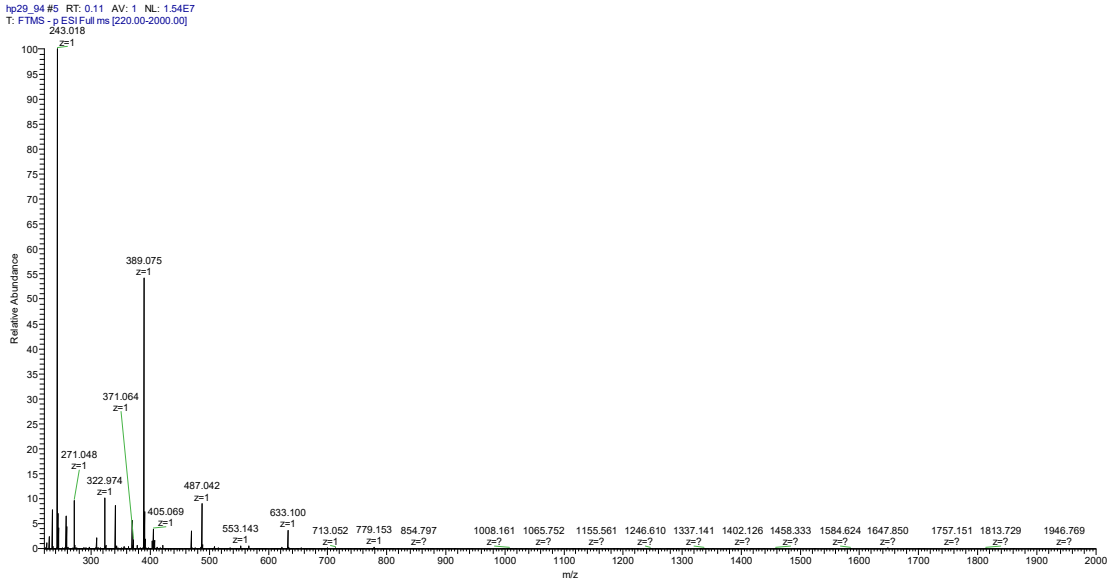

Figure S5. Negative-ion mode ESI-MS spectrum of Fraction 2 (Collected from 43-44 min).

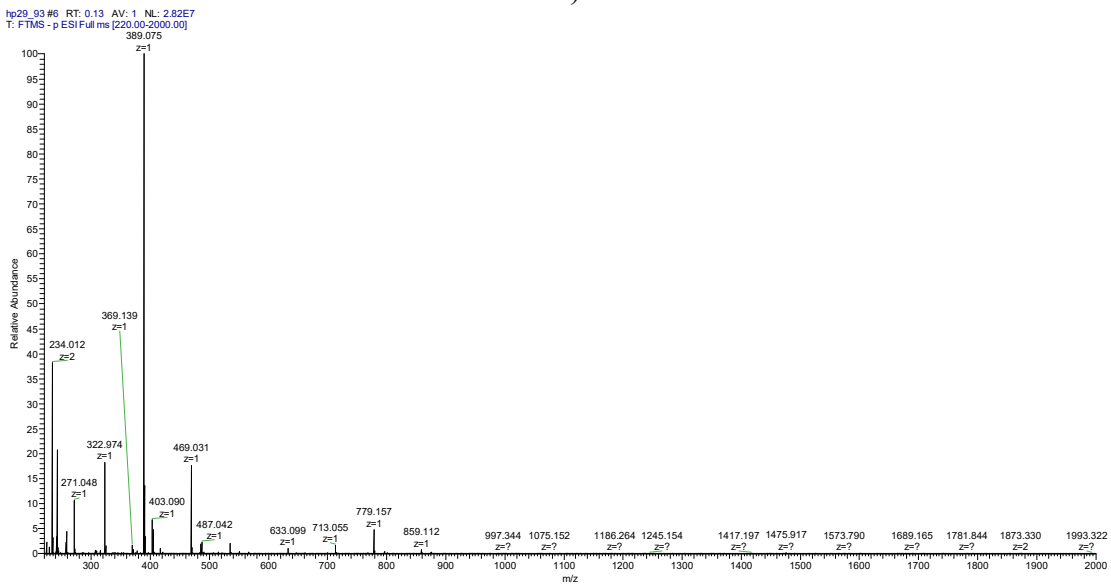

Figure S6. Negative-ion mode ESI-MS spectrum of Fraction 3 (Collected from 42-43 min).

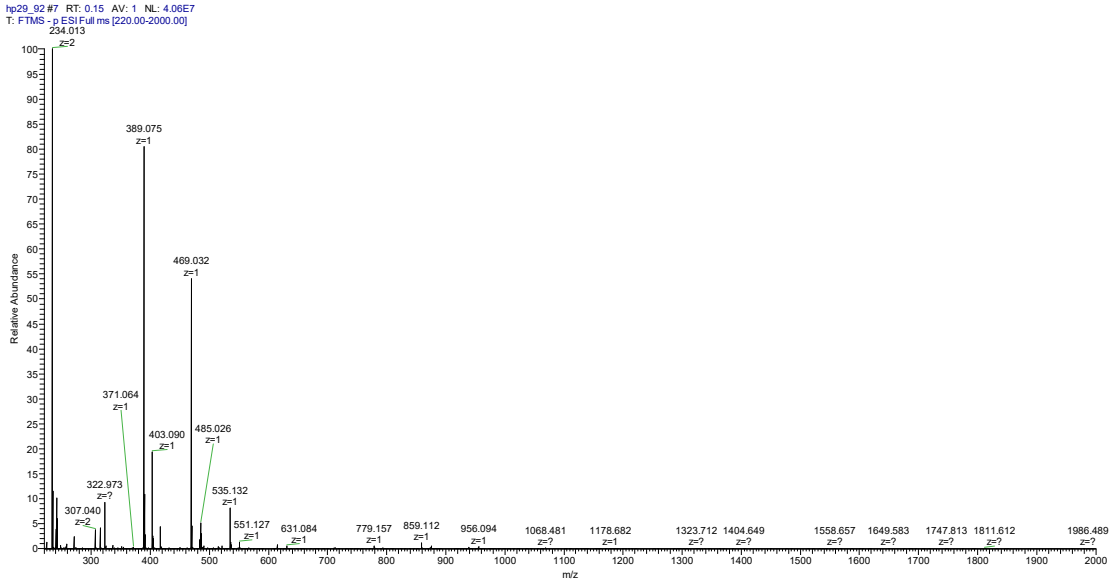

Figure S7. Negative-ion mode ESI-MS spectrum of Fraction 4 (Collected from 41-42 min).

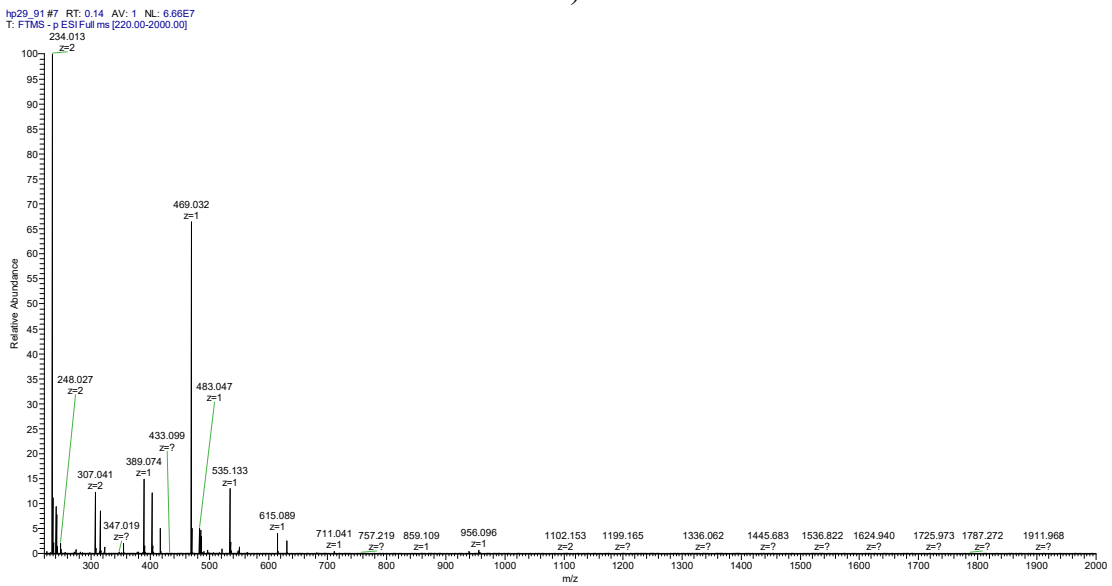

Figure S8. Negative-ion mode ESI-MS spectrum of Fraction 5 (Collected from 40-41 min).

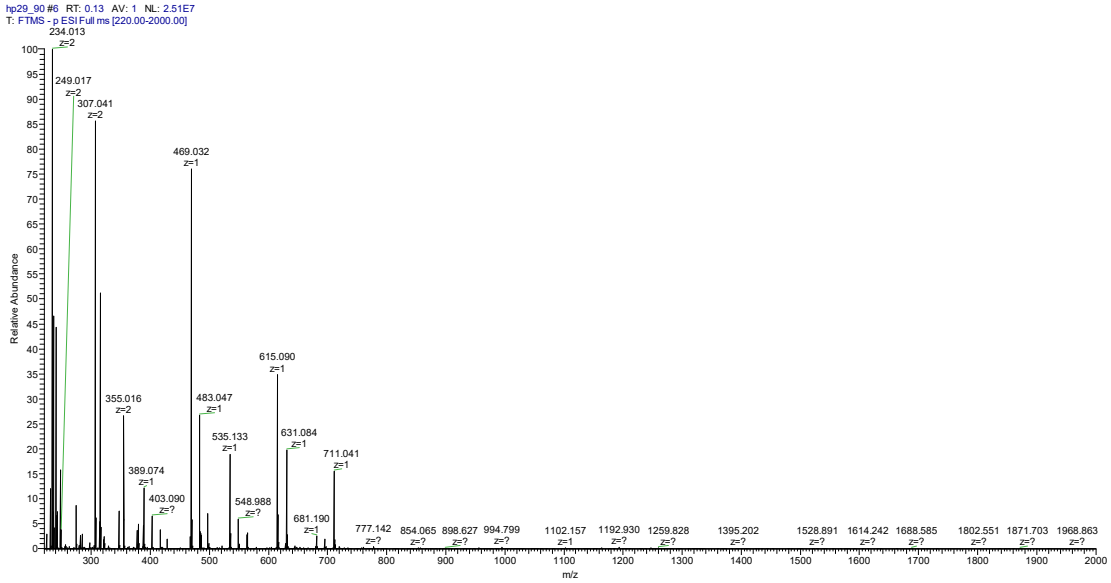

Figure S9. Negative-ion mode ESI-MS spectrum of Fraction 6 (Collected from 39-40 min).

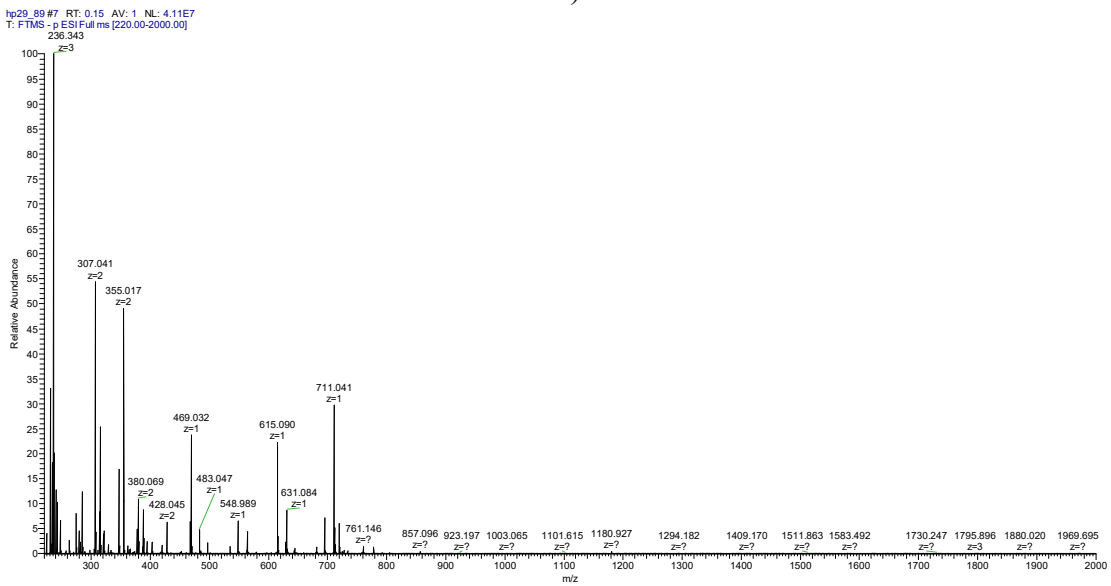

Figure S10. Negative-ion mode ESI-MS spectrum of Fraction 7 (Collected from 38-39 min).

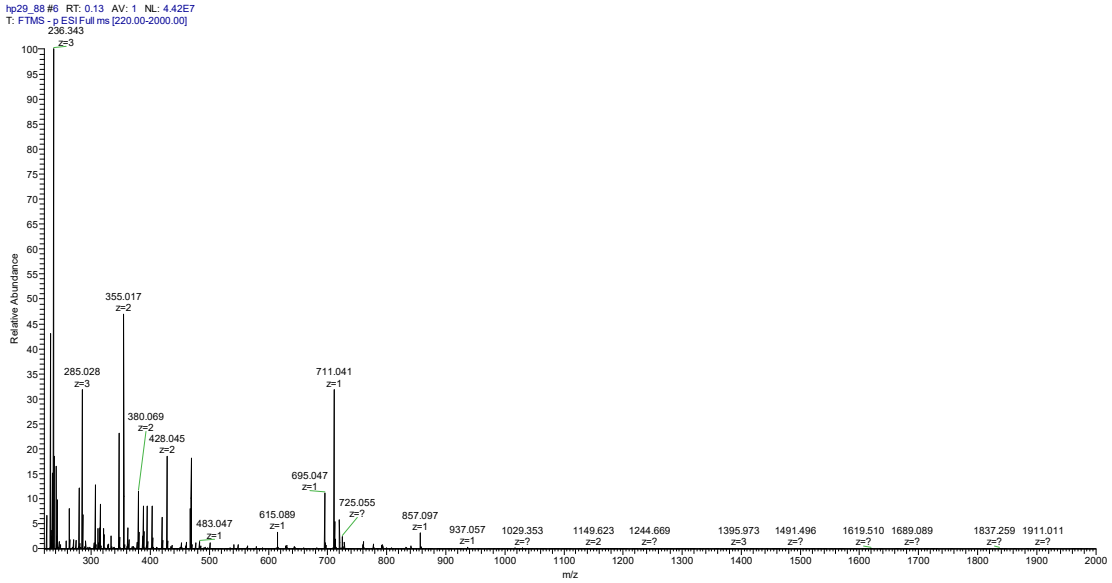

Figure S11. Negative-ion mode ESI-MS spectrum of Fraction 8 (Collected from 37-38 min).

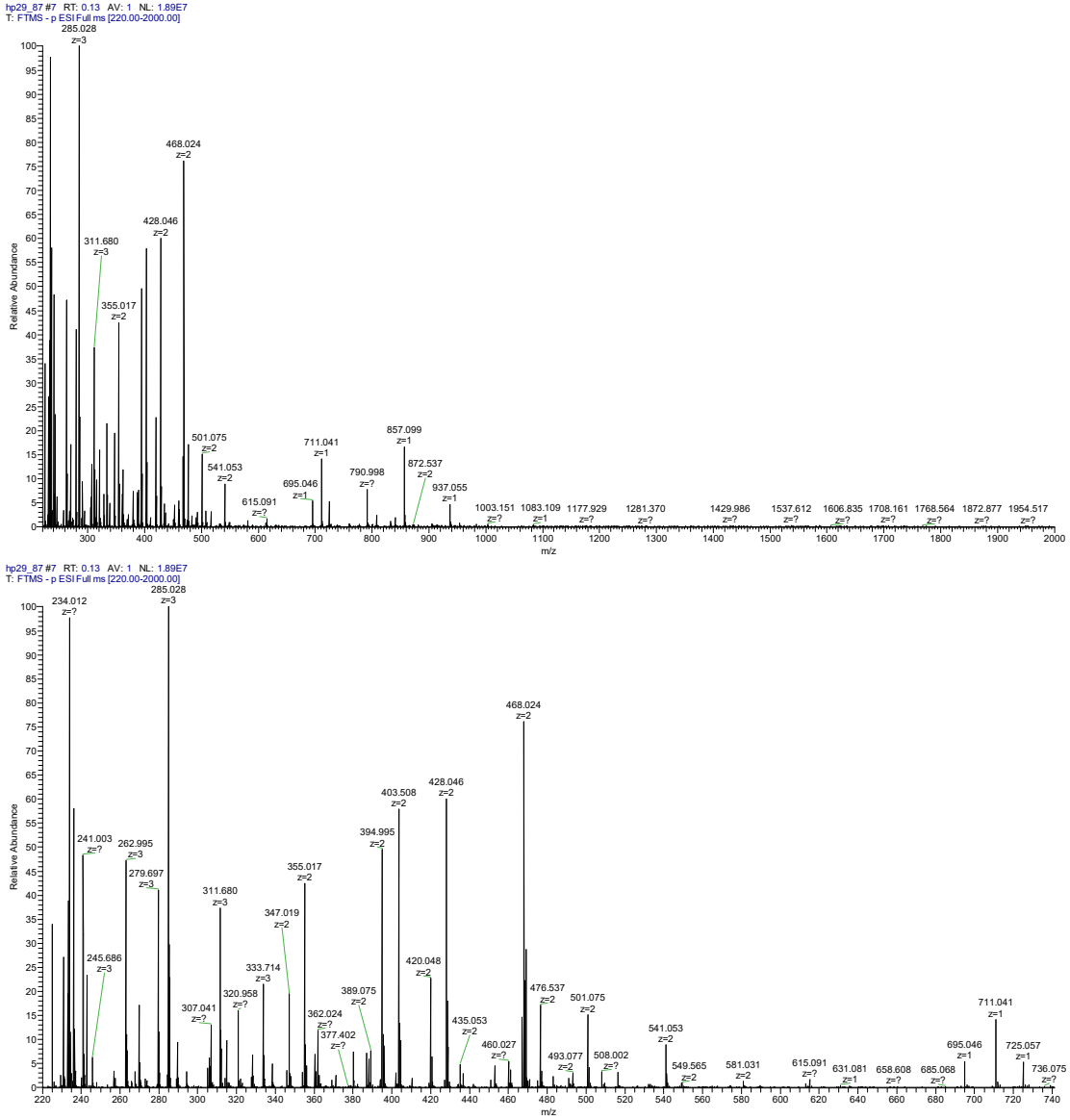

Figure S12. Negative-ion mode ESI-MS spectrum of Fraction 9 (Collected from 36-37 min).
(Top was the original spectrum and below was the expanded expanded spectrum).

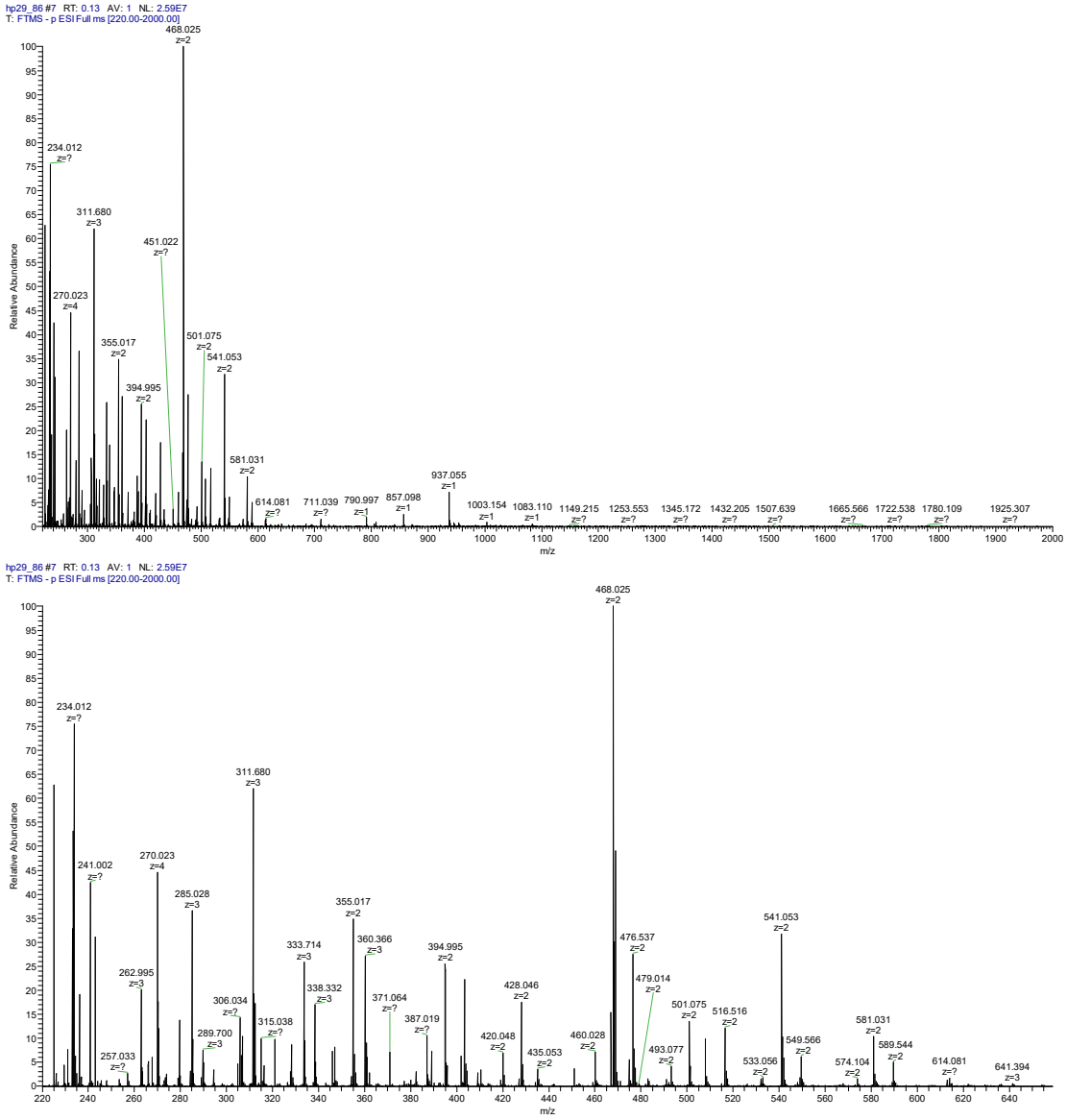

Figure S13. Negative-ion mode ESI-MS spectrum of Fraction 10 (Collected from 35-36 min).
(Top was the original spectrum and below was the expanded expanded spectrum).

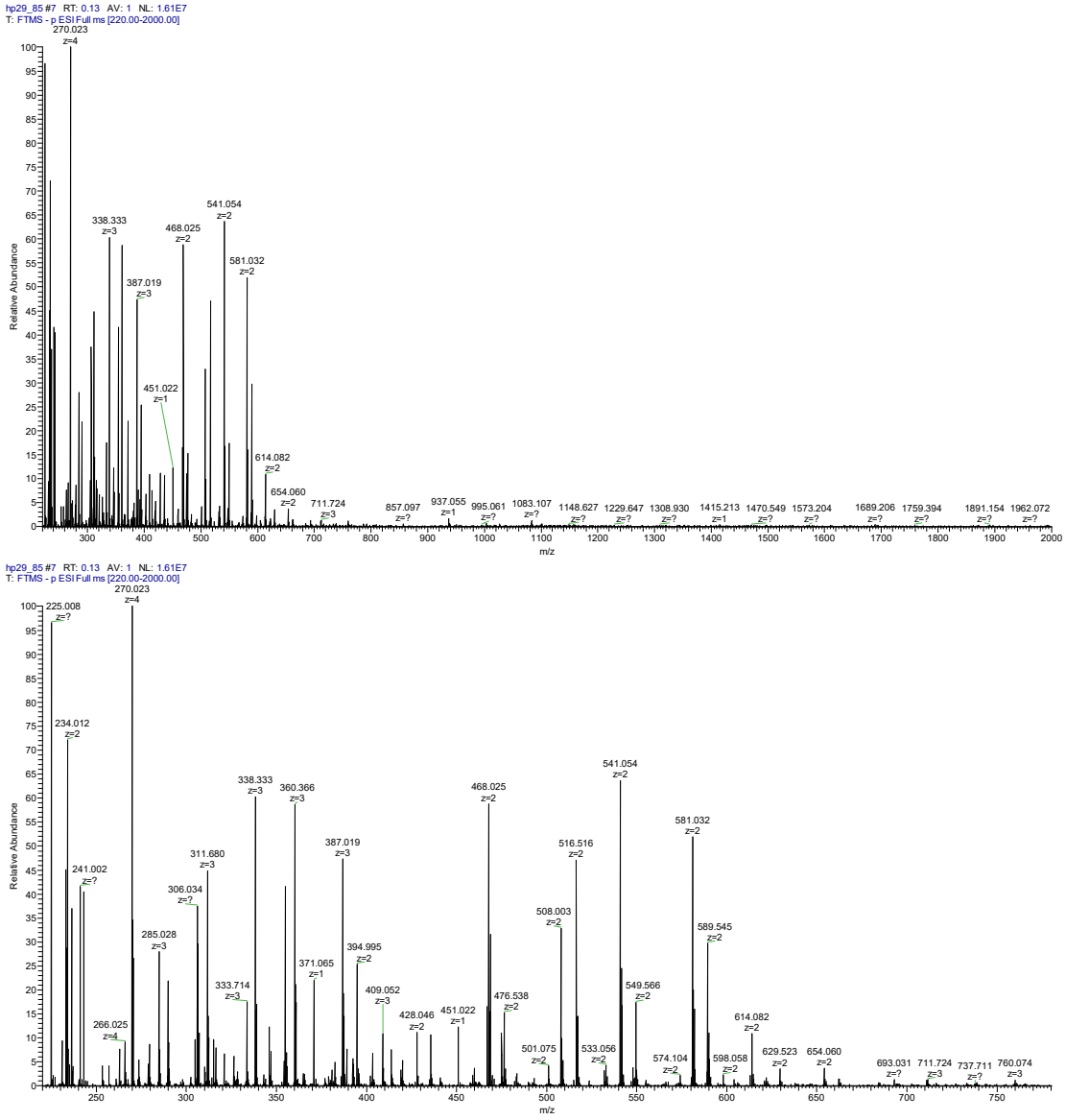

Figure S14. Negative-ion mode ESI-MS spectrum of Fraction 11 (Collected from 34-35 min) (Top was the original spectrum and below was the expanded expanded spectrum).

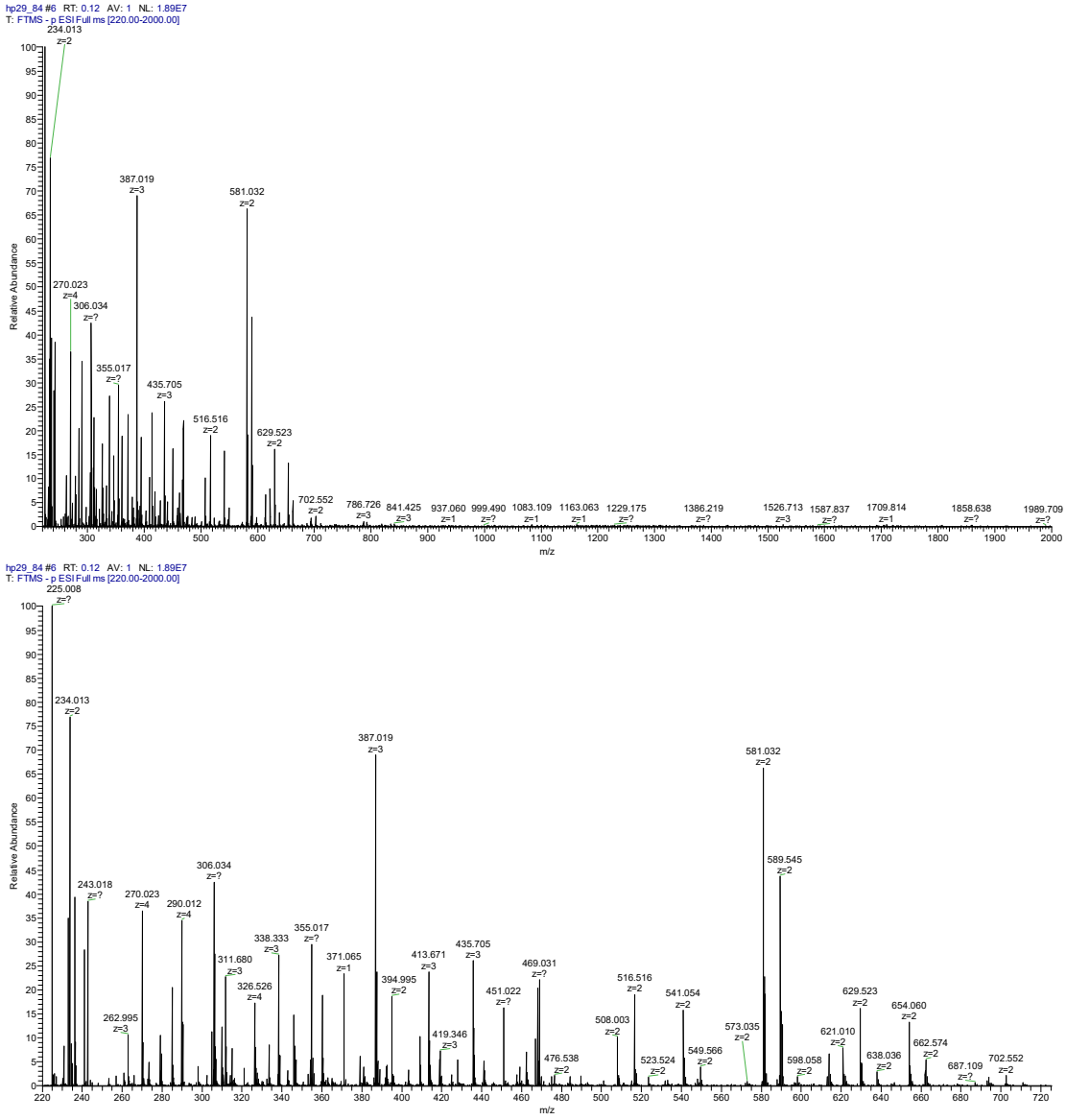

Figure S15. Negative-ion mode ESI-MS spectrum of Fraction 12 (Collected from 33-34 min).

(Top was the original spectrum and below was the expanded expanded spectrum).

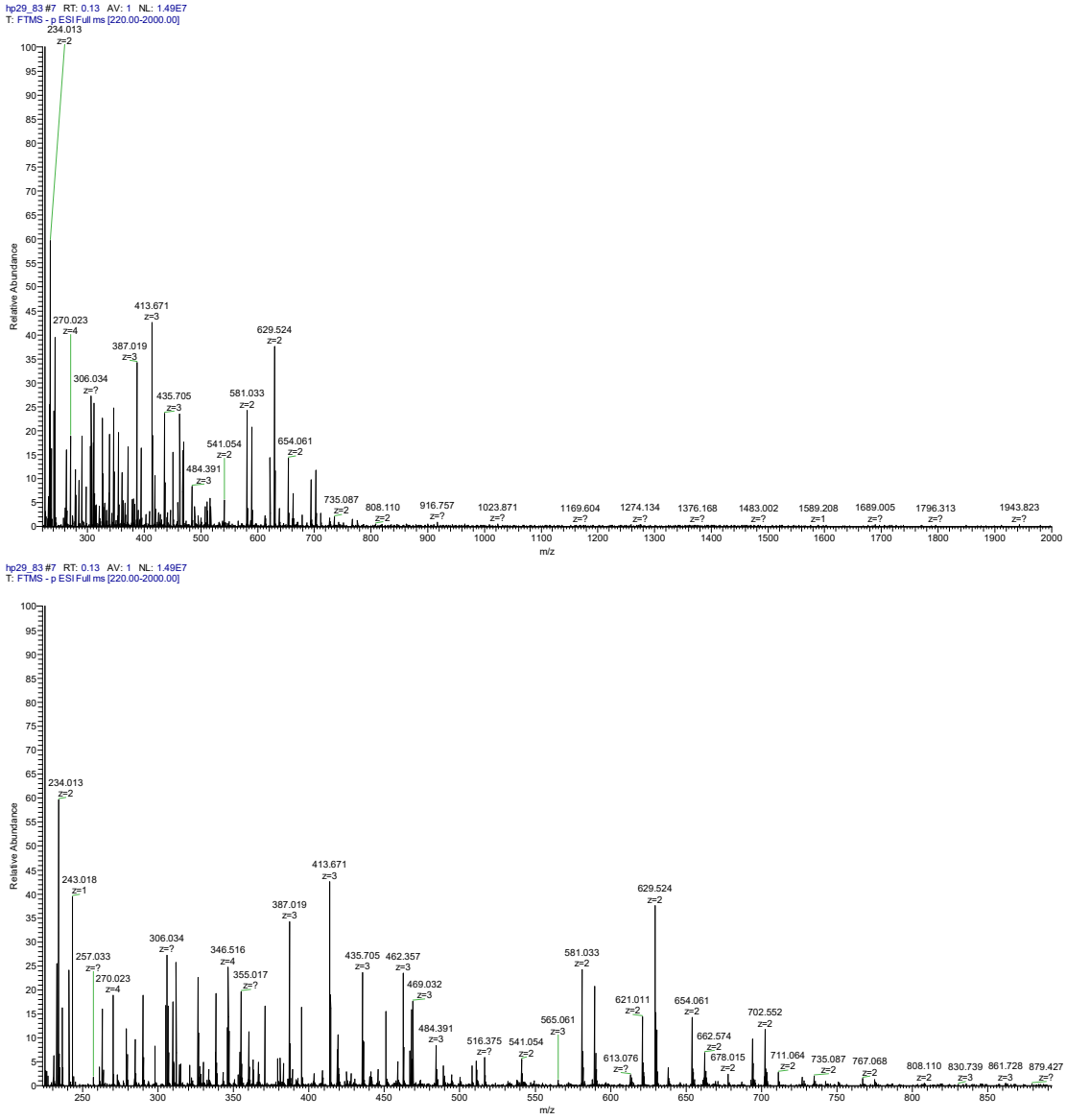

Figure S16. Negative-ion mode ESI-MS spectrum of Fraction 13 (Collected from 32-33 min). (Top was the original spectrum and below was the expanded expanded spectrum).

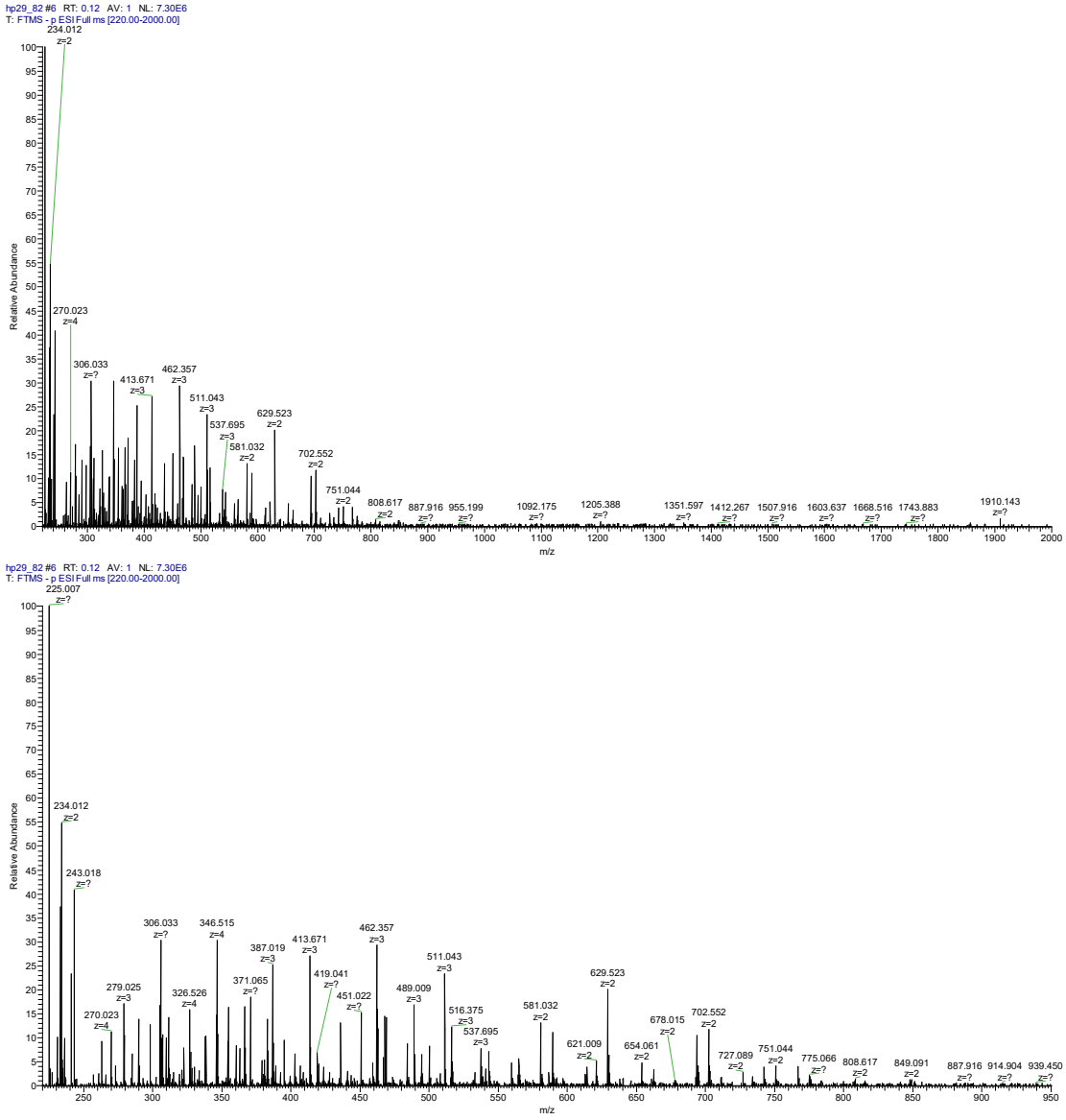

Figure S17. Negative-ion mode ESI-MS spectrum of Fraction 14 (Collected from 31-32 min). (Top was the original spectrum and below was the expanded expanded spectrum).

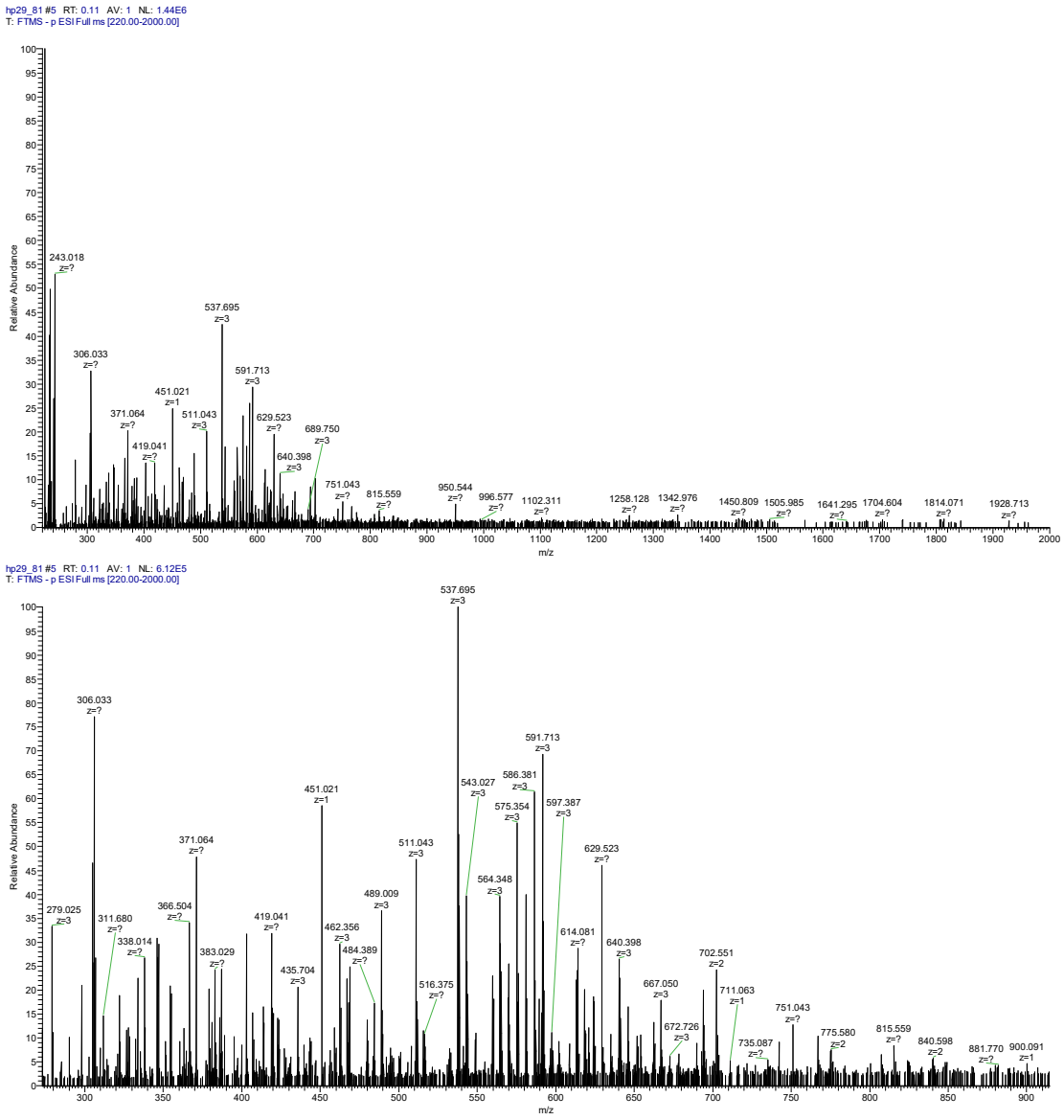

Figure S18. Negative-ion mode ESI-MS spectrum of Fraction 15 (Collected from 30-31 min). (Top was the original spectrum and below was the expanded expanded spectrum).

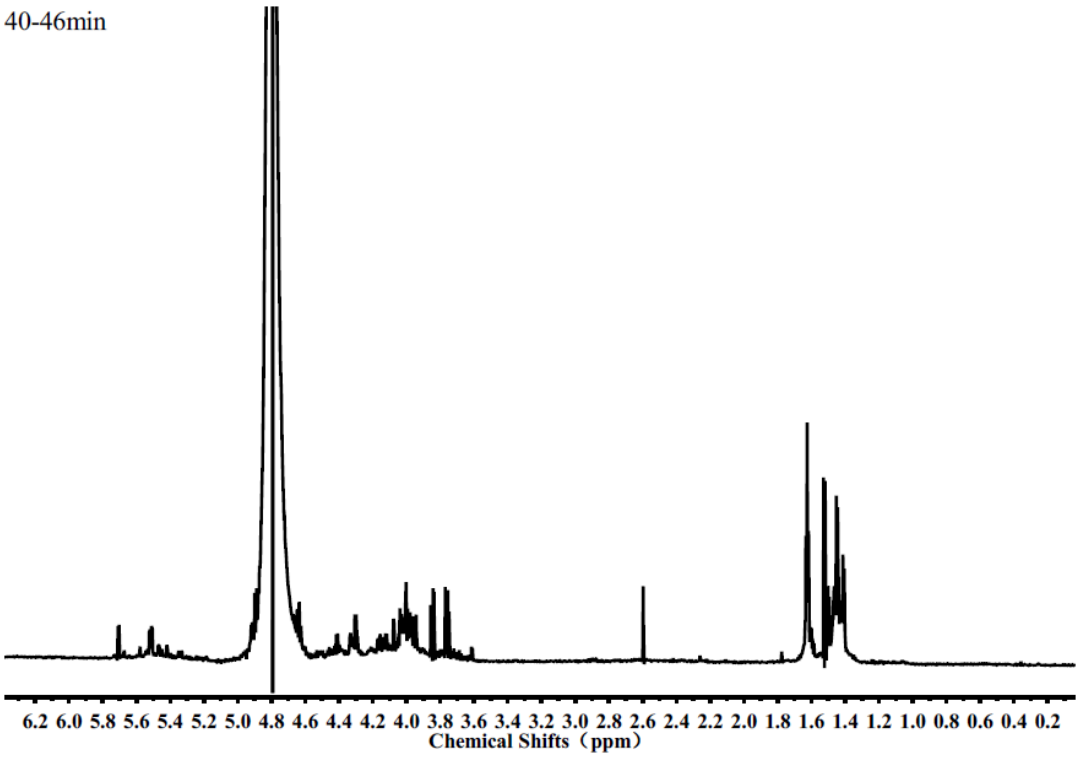

Figure S19. The ^{1}H NMR spectrum of Fraction 1 (Collected from 40-46 min).

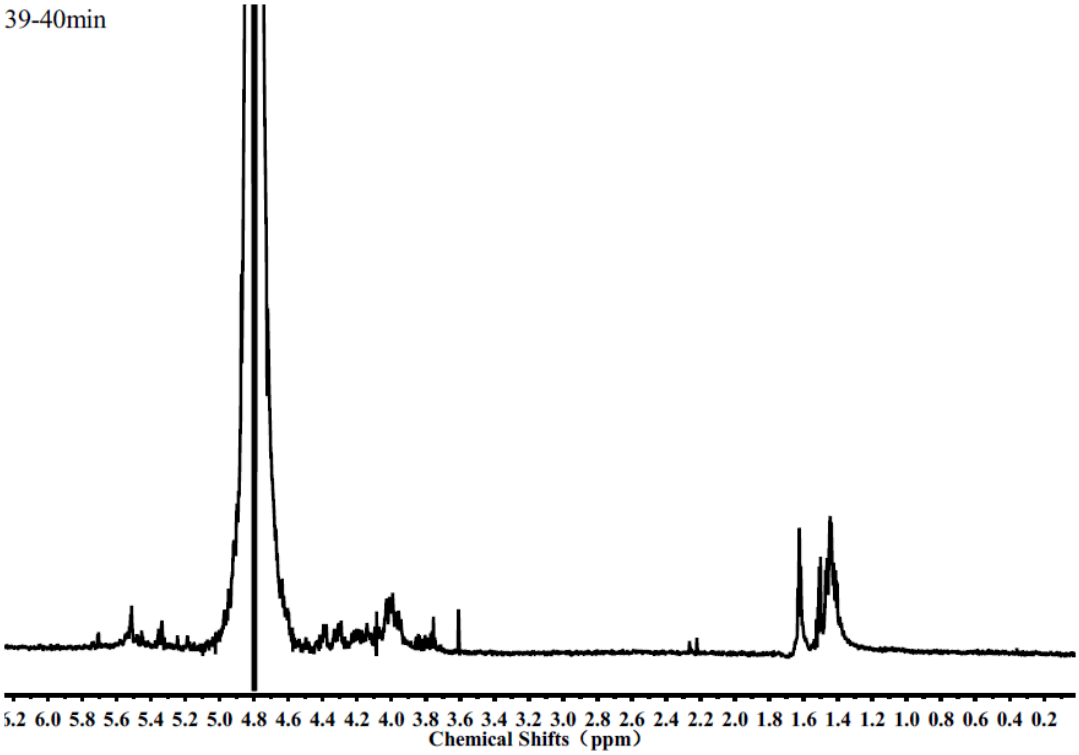

Figure S20. The ^{1}H NMR spectrum of Fraction 2 (Collected from 39-40 min).

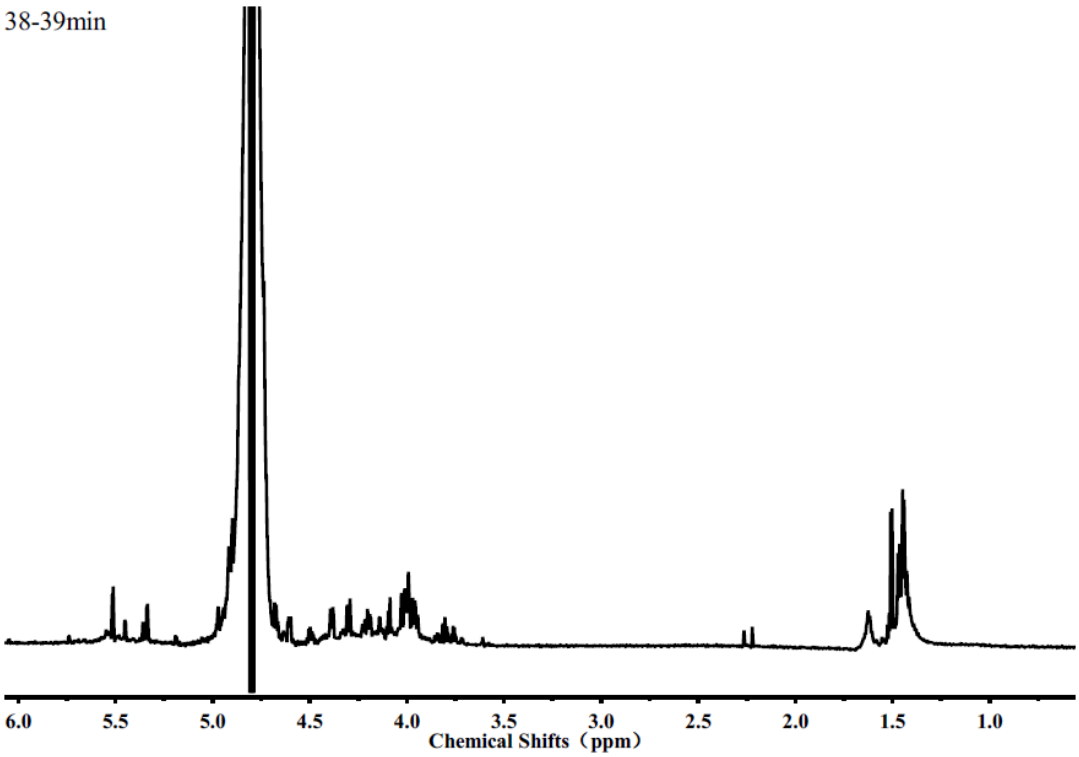

Figure S21. The ^{1}H NMR spectrum of Fraction 3 (Collected from 38-39 min).

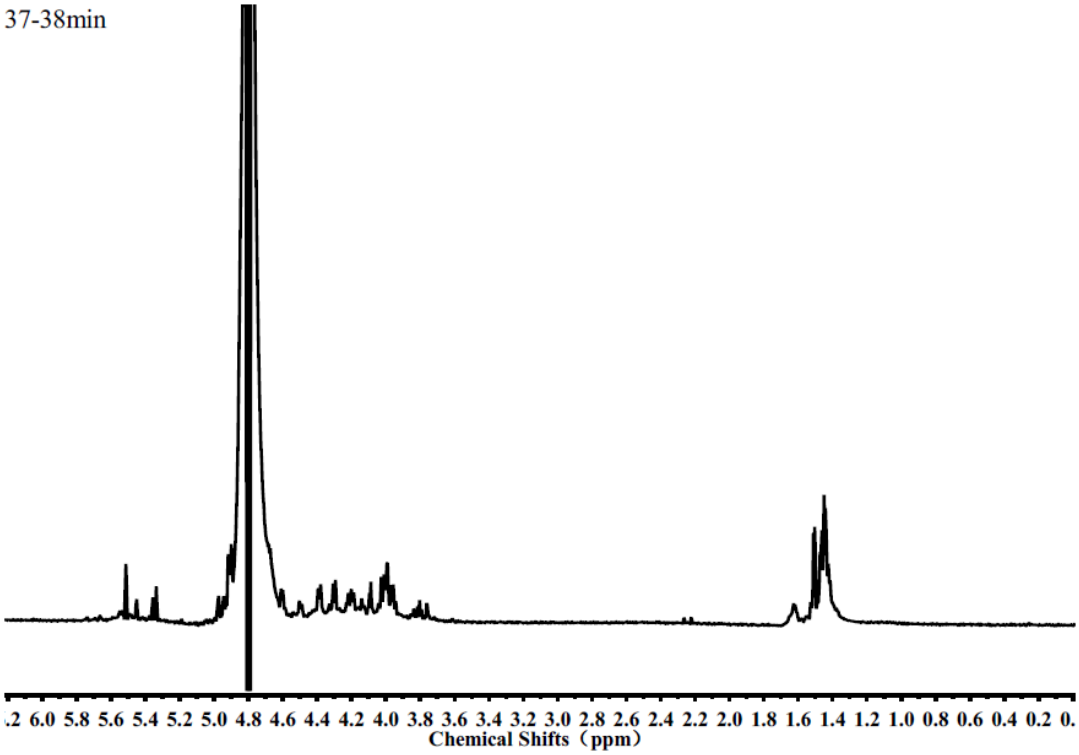

Figure S22. The ^{1}H NMR spectrum of Fraction 4 (Collected from 37-38 min).

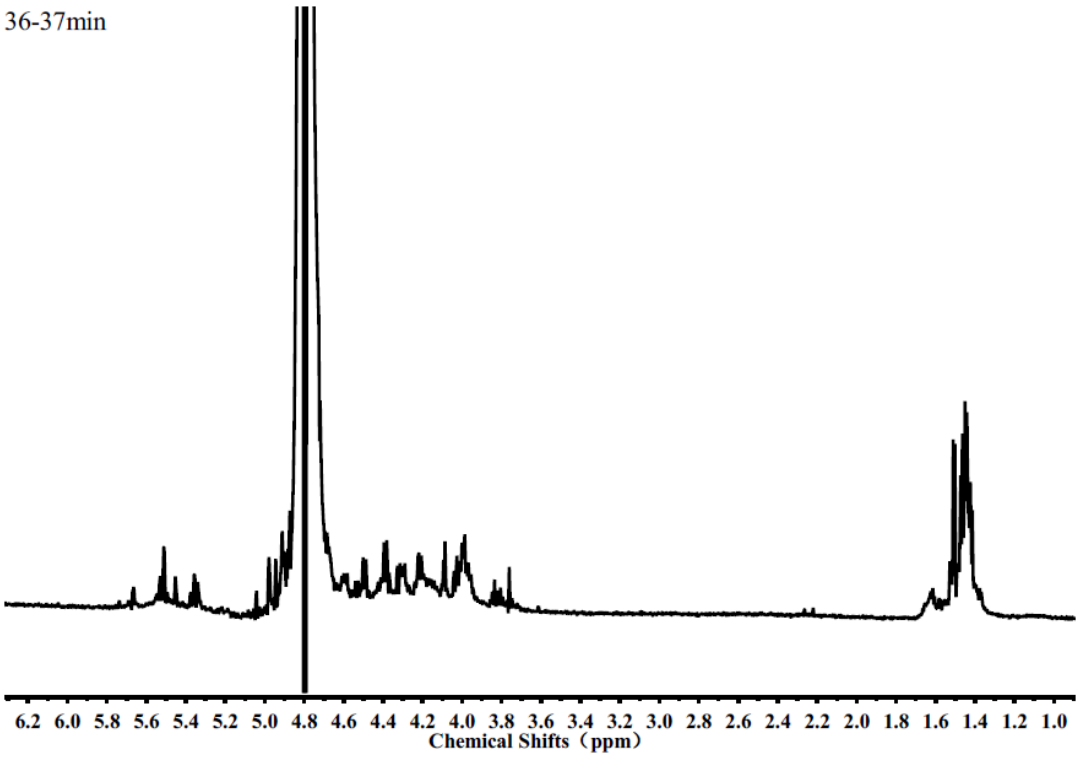

Figure S23. The ^{1}H NMR spectrum of Fraction 5 (Collected from 36-37 min).

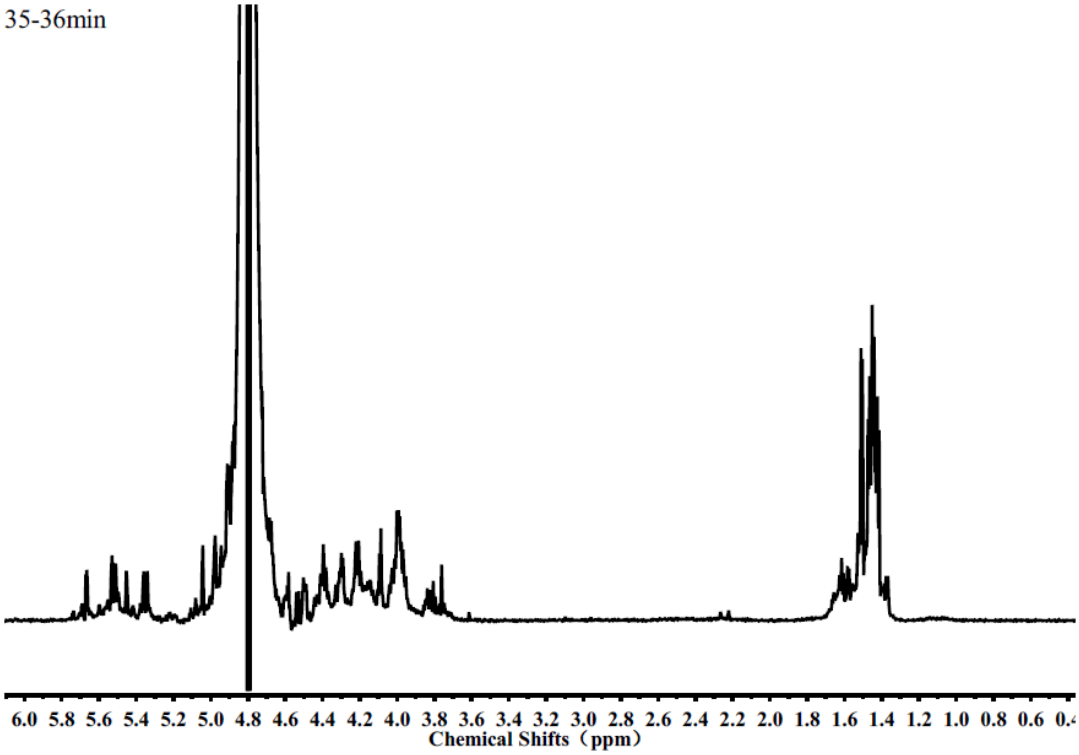

Figure S24. The ^{1}H NMR spectrum of Fraction 6 (Collected from 35-36 min).

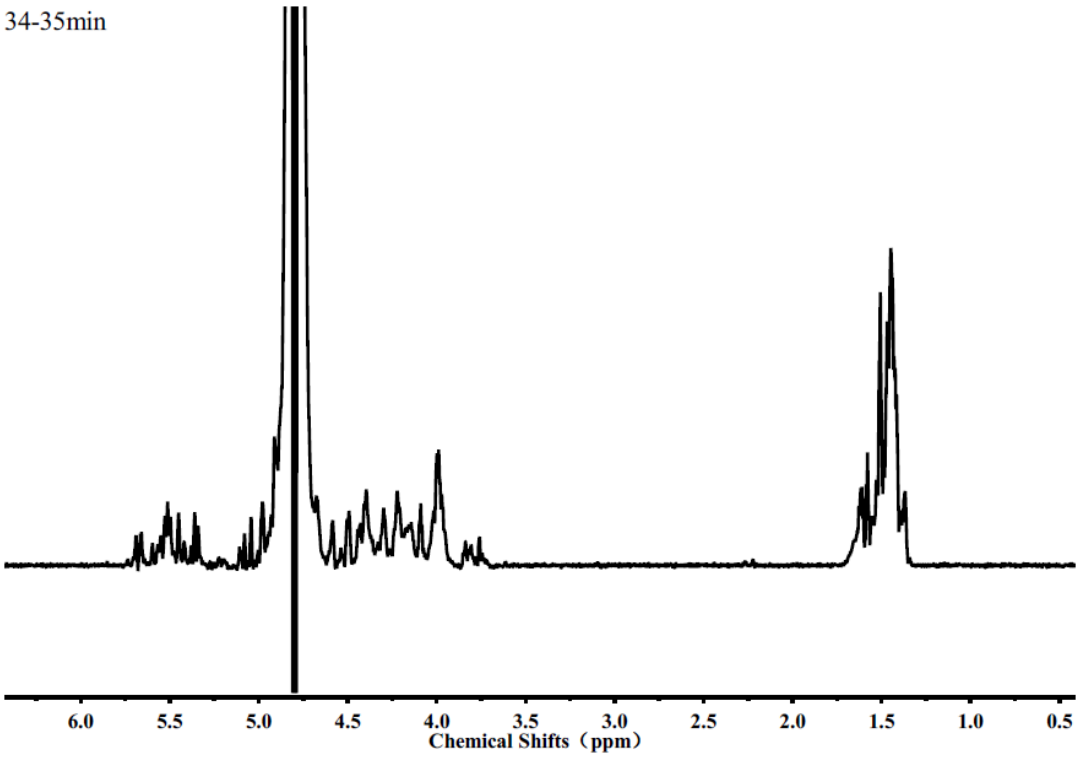

Figure S25. The ^{1}H NMR spectrum of Fraction 7 (Collected from 34-35 min).

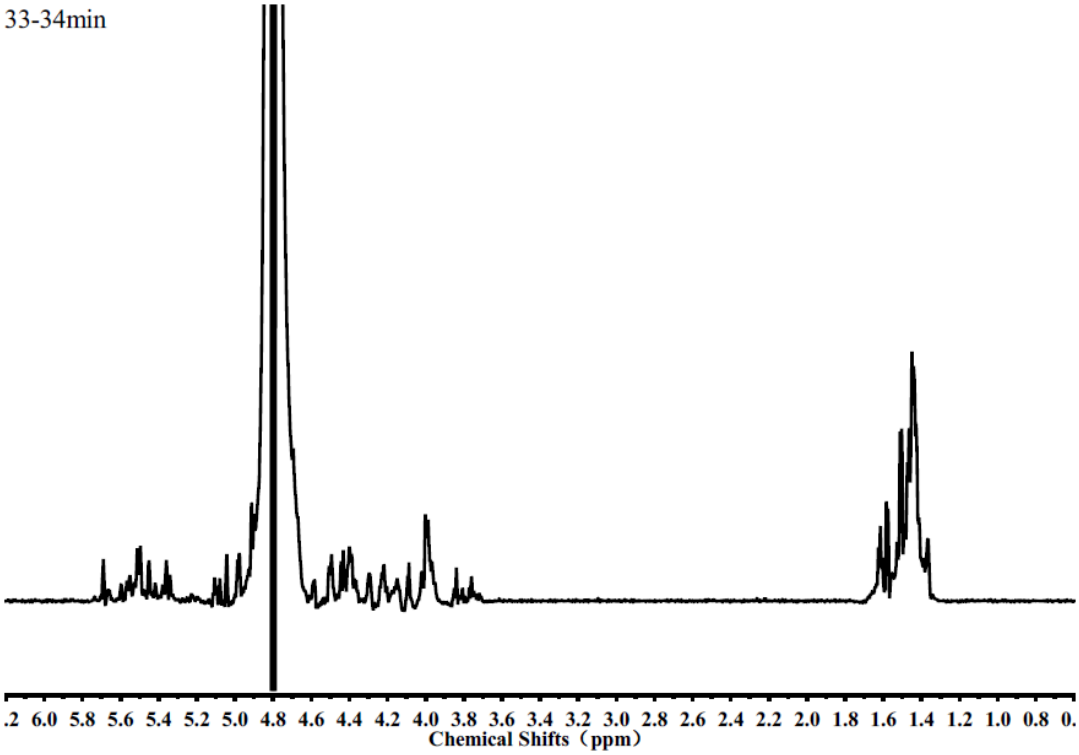

Figure S26. The ^{1}H NMR spectrum of Fraction 8 (Collected from 33-34 min).

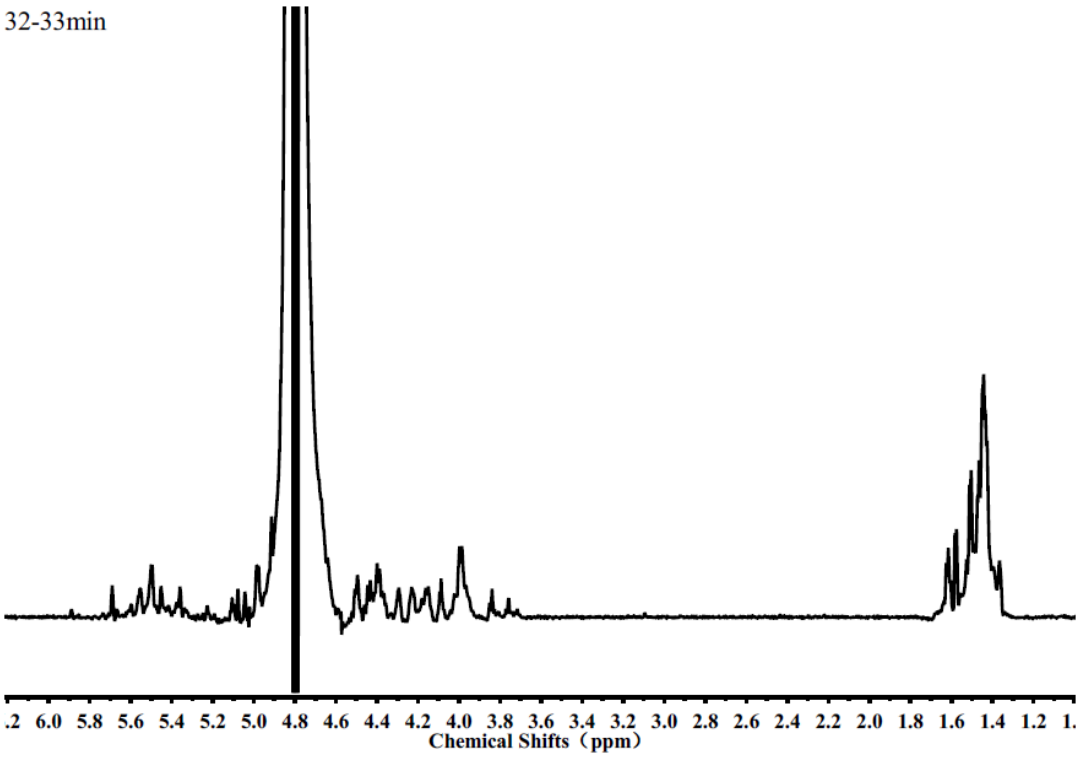

Figure S27. The ^{1}H NMR spectrum of Fraction 9 (Collected from 32-33 min).

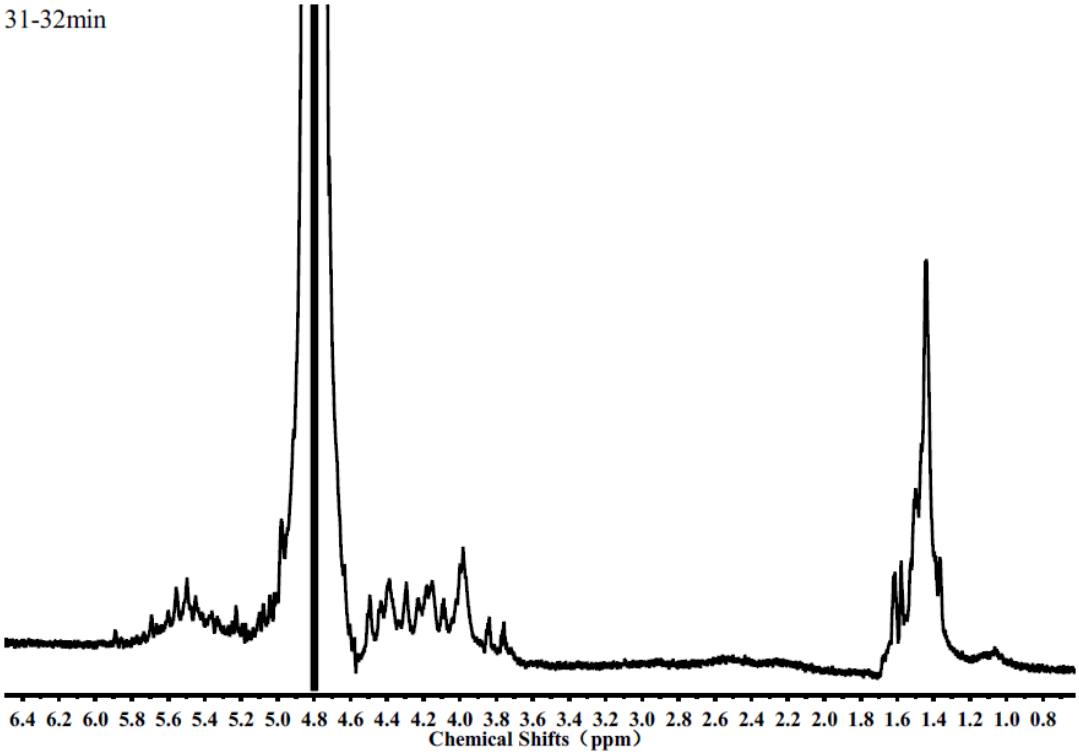

Figure S28. The ^{1}H NMR spectrum of Fraction 10 (Collected from 31-32 min).

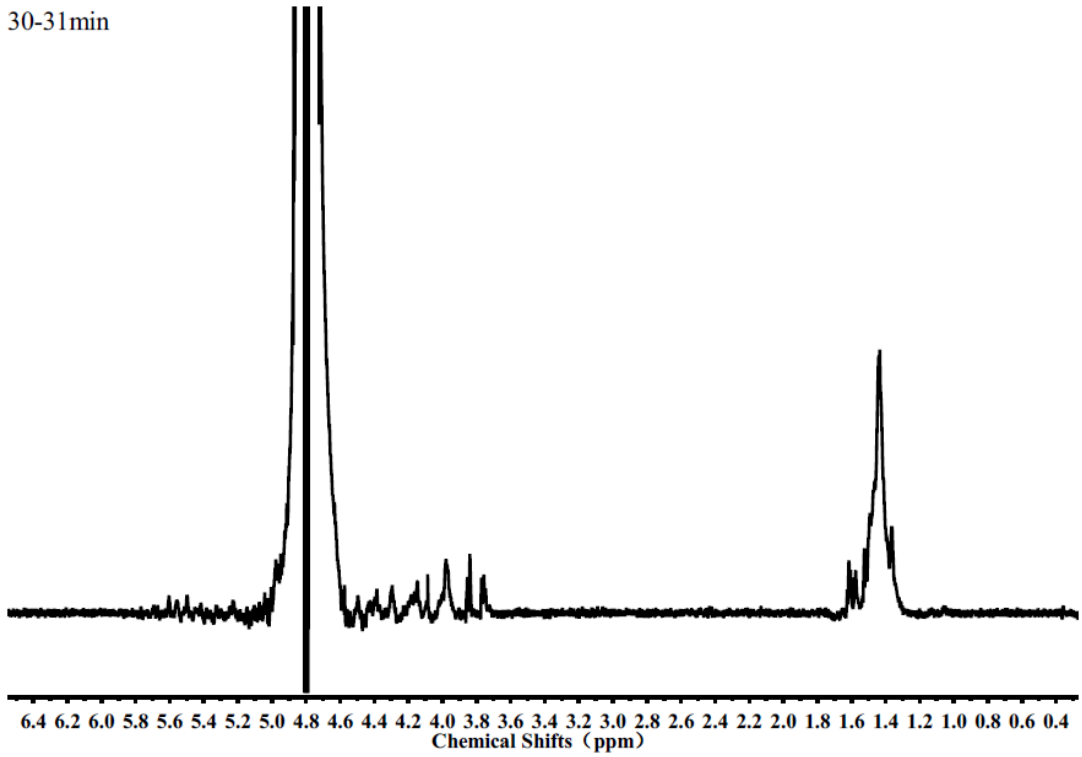

Figure S29. The ^{1}H NMR spectrum of Fraction 11 (Collected from 30-31 min).

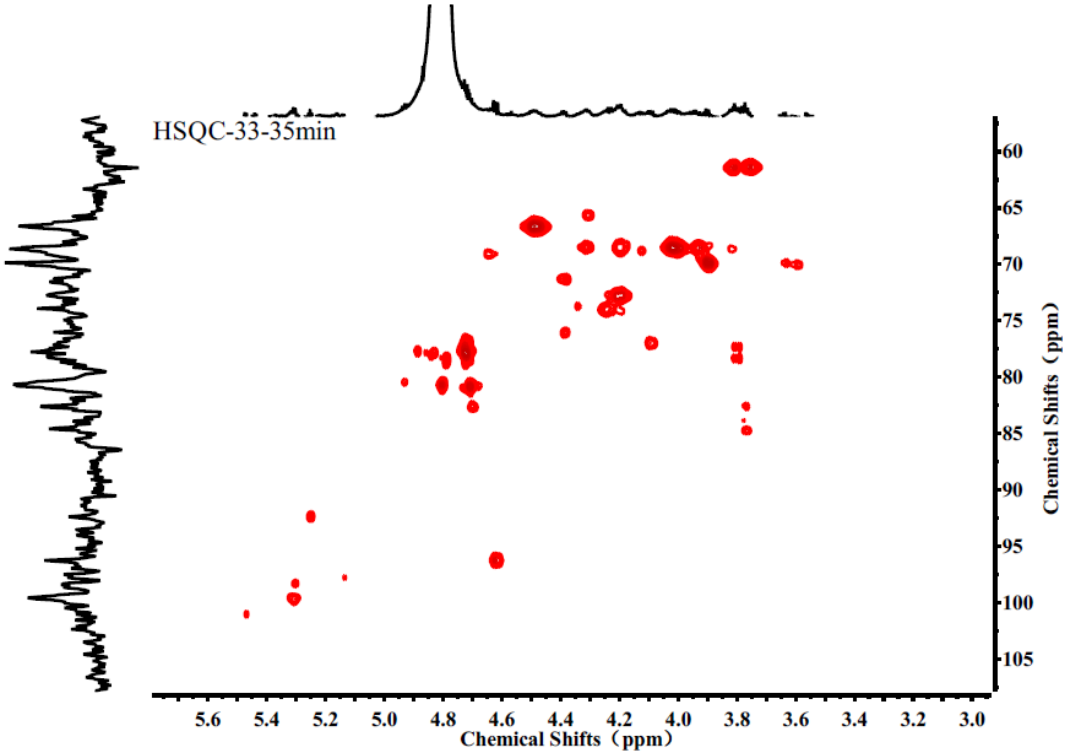

Figure S30. The HSQC spectrum of Fraction 7-8 (Collected from 33-35 min).

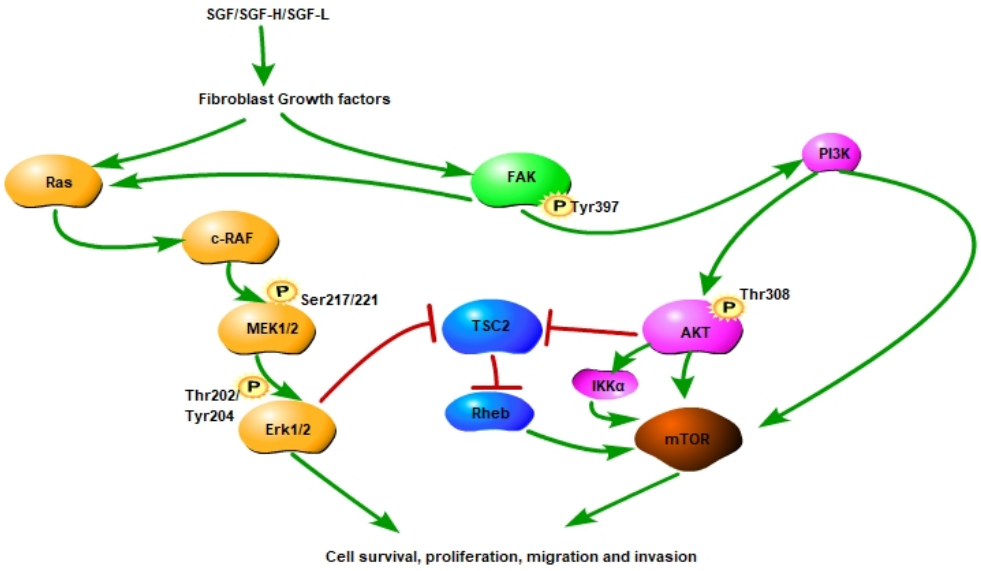

Figure S31. The mechanism of SGF, SGF-H and SGF-L exhibited the anti-lung cancer activity

Reference

1 W. Jin, W. Wu, H. Tang, B. Wei, H. Wang, J. Sun, W. Zhong, Structure Analysis and Anti-Tumor and Anti-Angiogenic Activities of Sulfated Galactofucan Extracted from *Sargassum thunbergii*. *Mar. Drugs.*, 2019, **17**, 52.